J Mol Model (2001) 7:201–206
DOI 10.1007/s008940100035

ORIGINAL PAPER

Mariano C. González-Lebrero · Adrián G. Turjanski
José A. Olabe · Darío A. Estrin

Structure, solvation, and bonding in pentacyano(L)ferrate(II) ions (L=aliphatic amine): a density functional study

Received: 23 January 2001 / Accepted: 8 May 2001 / Published online: 3 July 2001

Abstract Quantum chemical calculations using density functional theory have been carried out to investigate the influence of aqueous solvation on the structure and bonding in $[Fe(CN)_5L]^{3-}$ with L an aliphatic amine (ammonia, methylamine, hydrazine, and ethylenediamine). Gas phase equilibrium geometries were fully optimized at the generalized gradient approximation (GGA) level. Solvent effects were modeled within the DFT methodology by using a discrete electrostatic representation of the water molecules in the first solvation shell. For the hydrazine and ethylenediamine complexes in vacuum we found two internal hydrogen bonds between the terminal amino group hydrogens and two equatorial cyanide ligands. However, considering the first solvation shell, an open structure in which the terminal amino group is solvated by water molecules becomes more stable in the ethylenediamine case. Metal–L dissociation energies were computed in vacuum, taking the first solvation shell into account. The results obtained were compared with experimental kinetic data in aqueous solution in order to assess the role of solvation in the reactivity of these complexes.

Keywords Solvent effects · DFT · Transition metal complexes

Introduction

Performing accurate calculations on the structure, spectroscopy, and reactivity of transition metal compounds has been a very demanding problem in theoretical chemistry [1, 2] and considerable success has been achieved in recent years, [3] particularly for coordination compounds, which can be considered as isolated species in condensed phases. This is the case for many organometallic compounds or complexes containing ligands such as carbonyl or polypyridines, which show no tendency to engage in specific, donor–acceptor interactions with the solvent.

On the other hand, in many transition metal complexes the so-called second-sphere interactions have been shown to influence the chemical properties leading to strong solvatochromic shifts in the charge-transfer absorption bands as well as in the redox potentials associated with the metal centers. [4] Theoretical modeling of these systems is a much more challenging issue indeed since solvation effects should necessarily be taken into account.

Methods that include electron correlation effects are often required to treat transition metal systems. [5] Since traditional ab initio methods that include correlation effects scale as N^m with $m>5$ (N is the number of basis functions of the system), the corresponding calculations are computationally very demanding and impose serious limitations on the size of the system. An alternative approach to conventional ab initio methods is based on the use of density functional theory (DFT). DFT methodologies are very interesting from the computational point of view, since the time required scales as N^3, making these approaches ideally suited for large systems. DFT has proven to provide a reliable tool in the investigation of this type of transition metal systems. [6, 7]

In a previous study we used DFT coupled with a continuum solvation model to investigate the infrared spectra of the pentacyano(nytrosil)ferrate(II) ion dissolved in different media. [8] The calculations showed good agreement with experimental data obtained in non-acceptor, aprotic solvents. In aqueous solutions, however, deviations were found that were not accounted for by the dielectric continuum model used. The properties of the NO ligand were strongly influenced by the specific interactions of cyanides with the solvent, leading to internal electronic shifts favored by the coupled cyanide–iron–ni-

M.C. González-Lebrero · A.G. Turjanski · J.A. Olabe
D.A. Estrin (✉)
Departamento de Química Inorgánica,
Analítica y Química Física and INQUIMAE,
Facultad de Ciencias Exactas y Naturales,
Universidad de Buenos Aires, Ciudad Universitaria, Pabellón 2,
(C1428EHA) Buenos Aires, Argentina
e-mail: dario@q1.fcen.uba.ar
Fax: 54-11-4576-3341

trosyl framework. We also employed a more sophisticated combination of continuum and discrete solvation models to investigate the basicity of the uncoordinated nitrogen on pyrazine in the pentaammine(pyrazine)ruthenium(II) and pentacyano(pyrazine)ruthenate(II) ions. [9] We showed that both specific first shell and long-range interactions were important to describe the observed behavior.

The occurrence of specific donor–acceptor interactions between cyanides and the solvent is characteristic of many $[M^{II}(CN)_5L]^{n-}$ complexes (M=Fe, Ru, Os; L=aliphatic and aromatic ammines). [10, 11] These pentacyano–L ions have been extensively used in studies on the structure and reactivity of pseudooctahedral species, thanks to the availability of compounds for the three transition series, the ability of M to reach oxidation states II and III, and the widely accessible disposal of L ligands. [12]

In this work we investigate the structure and bonding of $[Fe^{II}CN)_5L]^{3-}$ with L=aliphatic mono- and diamines: ammonia, methylamine, hydrazine, and ethylenediamine, using a DFT methodology. In the next section we give details of the computational methodology. In the Results and discussion section we present the optimized structures and discuss the effects of the solvent on the conformation of the hydrazine and ethylenediamine complexes and on Fe–L dissociation bond energies. Finally, we present our conclusions.

Computational methodology

The calculations were performed using the Gaussian basis set implementation of density functional theory, given in the program *Molecole*. [13] The Kohn–Sham self-consistent procedure was applied for obtaining the electronic density and energy through the determination of a set of one-electron orbitals. [14] Gaussian basis sets were used for the expansion of the one-electron orbitals and also for the additional auxiliary set used for expanding the electronic density. Matrix elements of the exchange-correlation potential were calculated by a numerical integration scheme. [15] The double ζ plus polarization basis sets optimized by Sim et al. for DFT calculations were used for C, N, and H atoms. [16] For Fe the double ζ quality basis set basis sets given in [17] were used. The contraction patterns were (5211/411/1) for C and N, (4333/431/41) for Fe, and (41/1) for H. The contraction patterns for the electronic density expansion sets are (1111111/111/1) for C and N, (1111111111/111/111) for Fe, and (111111/1) for H. [16] A more detailed description of the technical aspects of the program is given in [13]. Computations were performed at the generalized gradient approximation (GGA) DFT level. The correlation part is composed of the parameterization of the homogeneous electron gas given by Vosko, [18] with the gradient corrections of Perdew. [19] The expression given by Becke for the gradient corrections in the exchange term has been used. [20] This level of theory has proved to be necessary for accurate evaluation of bond energies. [21]

Although the most obvious way to account for solute–solvent interactions in a theoretical calculation is to surround the molecule of interest with sufficient solvent molecules to represent the effects of bulk solvation, this approach is extremely expensive if electronic structure calculations are performed in the full system. Different continuum models have been used successfully for the calculation of ligand exchange reactions and electrode potentials. [22] However, as mentioned above, they may show deviations in cases in which specific interactions are important. We have implemented a hybrid discrete approach by treating the solute quantum mechanically and the remainder of the system by using classical force fields. Communication between the two parts of the system is allowed via electrostatic and van der Waals interactions. Several of these hybrid potentials have been implemented using semiempirical, ab initio, and DFT methods. [23] Within this scheme, we consider only the first shell of water molecules, modeled by using the hybrid discrete scheme described above and the four-site TIP4P potential for water. [24] Structural changes in complex geometry due to the solvent were neglected. Since many structures of nearly the same total energy are possible, we considered "typical" solvation structures. In all cases, the water molecules in the first solvation shell were chosen such as to solvate each cyanide with one hydrogen-bonded water molecule. The hydrogen bond distance (N cyanide–H donor) was constrained at a value of 1.5 Å. In the hydrazine complex, the structure with internally H-bonded hydrazine was solvated by one water molecule, acting as a donor to the uncoordinated nitrogen. The open structure was solvated with one water molecule acting as acceptor to one of the terminal hydrogen atoms. For ethylenediamine, the same solvation patterns were employed. Hydrogen bond distances were constrained at 2.0 Å (H amine–O water). In all cases, the free amines were solvated with the same number of water molecules as in the whole complex. The solvated structures are shown in Fig. 1C and D for $[Fe(CN)_5NH_3]^{3-}$ and $[Fe(CN)_5NH_2CH_3]^{3-}$, respectively; in Fig. 2C and D for the closed and open conformations of $[Fe(CN)_5N_2H_4]^{3-}$, respectively; and in Fig. 3C and D for the closed and open conformations of $[Fe(CN)_5en]^{3-}$, respectively.

Results and discussion

Optimized structures

Figure 1A and B shows the optimized geometries in vacuum for the $[Fe(CN)_5NH_3]^{3-}$ and $[Fe(CN)_5NH_2CH_3]^{3-}$ ions, respectively. The results for bond lengths are collected in Table 1. Experimental values of the structural parameters, obtained by X-ray diffraction experiments in $Na_3[Fe(CN)_5NH_3]\cdot 7H_2O$ are also presented in Table 1. [25] Our computed results are in good agreement with

Table 1 Computed bond distances (Å) for $[Fe(CN)_5L]^{3-}$ (L=NH_3, NH_2CH_3, N_2H_4, en). (c) and (o) stand for closed and open structures, respectively. Experimental X-ray information for $[Fe(CN)_5NH_3]^{3-}$ is also included (Fe–C_{eq} and C_{eq}–N_{eq} bond distances are averages)

Parameter	NH_3 (exp.)	NH_3	NH_2CH_3	N_2H_4 (o)	N_2H_4 (c)	en (o)	en (c)
Fe–C1	1.912	1.973	1.964	1.941	1.957	1.967	1.941
Fe–C2	1.912	1.963	1.963	1.940	1.950	1.952	1.955
Fe–C3	1.912	1.954	1.960	1.959	1.964	1.957	1.971
Fe–C4	1.912	1.964	1.968	1.953	1.971	1.964	1.957
Fe–C5	1.860	1.916	1.921	1.915	1.913	1.911	1.911
Fe–N6	2.071	2.162	2.130	2.171	2.147	2.161	2.123
C1–N1	1.155	1.195	1.196	1.197	1.196	1.195	1.196
C2–N2	1.155	1.195	1.195	1.193	1.195	1.195	1.196
C3–N3	1.155	1.195	1.196	1.195	1.198	1.194	1.193
C4–N4	1.155	1.195	1.196	1.195	1.198	1.194	1.195
C5–N5	1.159	1.194	1.195	1.192	1.194	1.193	1.195
N6–H1	0.887	1.030	1.027	1.034	1.019	1.029	1.033
N6–H2	0.910	1.028	1.026	1.033	1.016	1.030	1.032
N6–H3	0.976	1.028	–	–	–	–	–
N6–C6		–	1.466	–	–	1.466	1.477
C6–H3		–	1.109	–	–	1.117	1.125
C6–H4		–	1.107	–	–	1.115	1.109
C6–H5		–	1.127	–	–	–	–
N6–N7		–	–	1.457	1.427	–	–
N7–H3		–	–	1.035	1.037	–	–
N7–H4		–	–	1.035	1.036	–	–
C6–C7		–	–	–	–	1.539	1.544
C7–N7		–	–	–	–	1.498	1.464
N7–H7		–	–	–	–	1.037	1.045
N7–H8		–	–	–	–	1.036	1.043
C7–H5		–	–	–	–	1.118	1.119
C7–H6		–	–	–	–	1.120	1.121

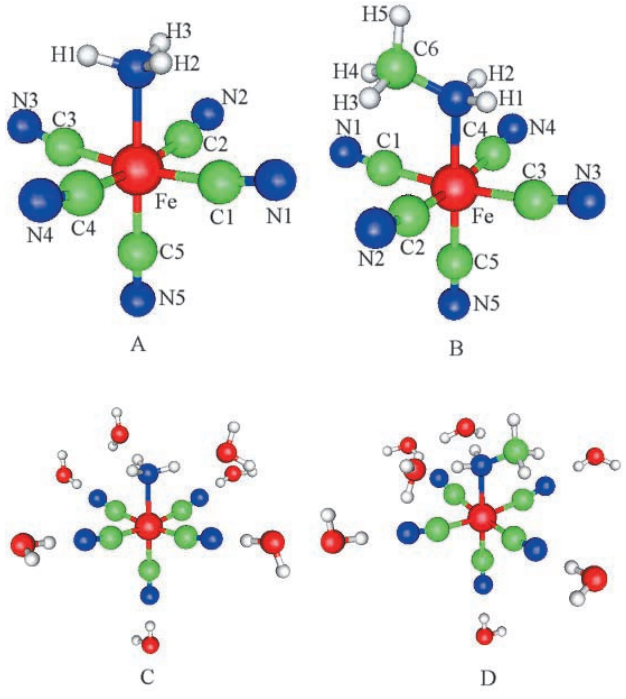

Fig. 1 Structures of isolated and solvated $[Fe(CN)_5NH_3]^{3-}$ and $[Fe(CN)_5NH_2CH_3]^{3-}$

experiment regarding bond distances and angles, and they show the systematic errors typical of DFT-GGA calculations. [26]

The geometries are, as expected, close to octahedral. However, there is a considerable deviation from planarity of the equatorial cyanides. The ($N_{eq}C_{eq}Fe$) angles range from 169° to 171° and from 171° to 173° in the ammonia and methylamine complexes, respectively. The optimized geometry of $[Fe(CN)_5]^{3-}$ shows less deviations from planarity ($N_{eq}C_{eq}Fe$ angles ranging from 173° to 176°). Since the consideration of only steric and electrostatic effects would lead to a larger deviation of planarity in the $[Fe(CN)_5]^{3-}$ complex compared to $[Fe(CN)_5L]^{3-}$ (L=NH_3, NH_2CH_3), we can ascribe this effect to the formation of weak hydrogen bonds between the ammonia and methylamine hydrogen atoms with the equatorial cyanides in vacuum. Distances between hydrogen atoms belonging to the ammonia or methylamine and terminal cyanide nitrogen atoms are about 3 Å; longer than in normal H bonds, but still sufficiently short to produce a noticeable effect. This explanation is also consistent with the fact that DFT calculations performed in $[Fe(CN)_5L]^{3-}$ complexes for L=aromatic amines predicted almost octahedral geometries. [11] Of course this observation correspond to isolated systems, and since the effect is weak, the environment may affect it significantly, as can be seen in the $Na_3[Fe(CN)_5NH_3]\cdot 7H_2O$ solid state experimental results, which show almost no deviations from planarity of the equatorial cyanides. [25]

The computed Fe–N distances are 2.162 and 2.130 Å for the ammonia and methylamine complexes, respectively. This is consistent with a stronger Fe–N bond, which is expected due to the larger basicity and proton affinity of methylamine compared with ammonia. [27, 28] The Fe–C5 (axial) bond length is significantly shorter than Fe–C (equatorial) ones in both cases; this was also noted in calculations of $[Fe(CN)_5L]^{n-}$ complexes,

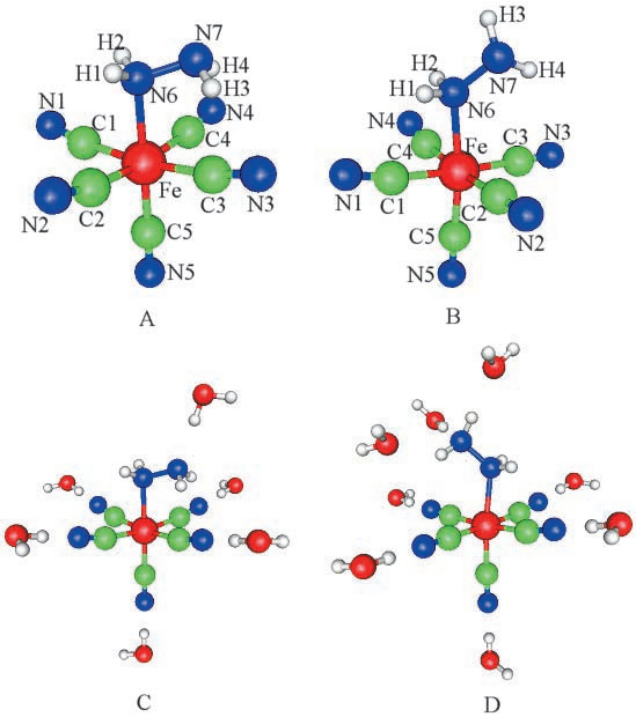

Fig. 2 Structures of closed and open conformations of isolated and solvated $[Fe(CN)_5N_2H_4]^{3-}$

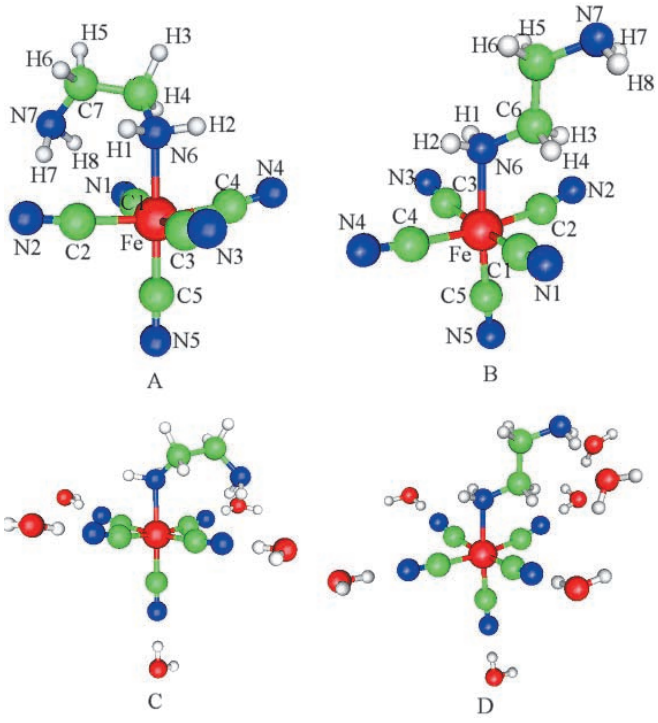

Fig. 3 Structures of closed and open conformations of isolated and solvated $[Fe(CN)_5en]^{3-}$

with L an N-heterocyclic base and in $[Fe(CN)_5NO]^{2-}$. [8, 11]

Figure 2A and B shows the structures of the closed and open conformations of $[Fe(CN)_5N_2H_4]^{3-}$, respectively. The closed conformation is the only stable structure in vacuum. By including two water molecules coordinated to the terminal hydrazine hydrogen atoms in the calculation, a second minimum corresponding to an open structure, 15.3 kcal mol^{-1} less stable than the closed conformation, can be characterized. Fe–C and C–N bond distances are similar to those computed in the ammonia and methylamine complexes. Overall, bond distances in the two conformations are quite similar, except the Fe–N distance; which is shorter in the closed structure. The computed value for the open structure is close to that computed in the amino complex; this is consistent with the similar values of proton affinity for ammonia and hydrazine. [28] In the closed structure, the cyanides involved in the strong intramolecular H bonds give longer C–N distances than the others. This can be ascribed to the stabilization of the negative charge in the cyanides due to the H bonds, leading to a larger degree of π^* back-donation. In turn, this leads to a larger degree of N_2H_4 σ-donation, and thus to a stronger and shorter Fe–N bond. This is consistent with the computed Mulliken populations. In the closed conformation the net charge donation from hydrazine is 0.159 *e*, while in the open structure it is 0.110 *e*.

Figure 3A and B shows the structures of the closed and open conformations of $[Fe(CN)_5en]^{3-}$, respectively. In this case, the two conformations were predicted to be stable both in vacuum and considering the first solvation shell. Remarkably, we have noted that the structure with internal hydrogen bonding is 6.2 kcal mol^{-1} more stable than the open conformer in vacuum, but taking into account the first solvation shell, the open conformation becomes 6.3 kcal mol^{-1} more stable than the closed one, due to the fact that solvation of both cyanides and hydrazine competes favorably with the internal hydrogen bonding. The Fe–C and C–N distances follow the same trends as in the complexes described previously, as well as the Fe–N bond length, which is also shorter in the closed conformation, compared to the open one. It can also be noted that N–H bond distances of H atoms involved in intramolecular hydrogen bonds are 1.045 Å, considerably longer than those computed in isolated ethylenediamine and in the open conformer, of 1.032 Å and 1.037, respectively.

Fe–L bond dissociation energies

We have performed calculations of the bond dissociation energies of the amino ligands, which correspond to the reaction enthalpy of the process:

$$[Fe(CN)_5L]^{3-} \rightarrow [Fe(CN)_5]^{3-} + L \quad (1)$$

We have neglected zero point energies and thermal corrections. The computed values in vacuum correspond to a situation in which there are no interactions with the environment. The results are collected in Table 2. The bond

Table 2 Fe–L bond dissociation energies (kcal mol^{-1}) in vacuum and including the effects of the first solvation shell for $[Fe(CN_5)L]^{3-}$ with L=NH_3, NH_2CH_3, N_2H_4 and en.Experimental values are activation enthalpies

	NH_3	NH_2CH_3	N_2H_4	en
Vacuum	10.5	12.9	25.2	23.1
Solution	14.1	15.1	22.3	22.0
Experimental	24.4[a]	24.7[a]	25.6[b]	24.4[c]

[a] From [29a] [b] From [29b] [c] From [29c]

dissociation energies in vacuum, considering the most stable conformations in each case, follow the trend: (hydrazine>en>methylamine>ammonia). The values computed for hydrazine and en are similar and much larger that the ones computed for the monoamines. This is due to the intramolecular hydrogen bonds present in the diamine complexes. The computed value for methylamine is larger than the one predicted for ammonia, as expected for a shorter (stronger) bond (see above).

Ligand substitution reactions of pentacyanoferrate(II) complexes

$$[Fe(CN)_5L]^{3-}+L' \rightarrow [Fe(CN)_5L']^{3-}+L \quad (2)$$

have been the subject of many mechanistic investigations. [29, 30, 31, 32] Experimental information is consistent with a dissociative mechanism for ligand substitution in these complexes. This means that ligand substitution involves the formation of an intermediate and is controlled by the nature of the leaving group L. In the Fe(II) case, it has been postulated that the intermediate is $[Fe(CN)_5]^{3-}$. [31] The activation enthalpies in aqueous solution have been found to be 24.4, 24.7, 25.6, and 24.4 kcal mol^{-1} for ammonia, methylamine, hydrazine, and en, respectively. [29] It can be noted that experimental activation energies are quite similar for all the amines considered, in contrast with the computed bond dissociation energies in vacuum. Considering that DFT provides estimates for bond dissociation energies in good agreement with experimental results for transition metal systems in the gas phase, [33] we infer that the large differences between computed bond dissociation energies in vacuum and experimental activation energies can be accounted by considering solvent effects. This is not surprising, since it is well known that the environment affects reactivity and spectroscopic properties of many related systems profoundly. [8, 11, 13, 16, 34]

A quantitative analysis of solvation effects on the dissociation reaction would require performing simulations in which the free energy profile or potential of mean force is evaluated using a quantum mechanical description of the complex. Since this is beyond the scope of this article because of the large computational cost of such a simulation, we have performed a series of single point calculations for both the products and reactants in reaction (1). We have considered the solvent molecules in the first solvation shell explicitly, according to the methodology described above. Using this approach, the results obtained for Fe–L bond dissociation energies in all cases tend to get closer to the experimental results. The increase of bond dissociation energies in the monoamine complexes upon solvation is related to the more favorable solvation of the ligands in the complex compared to $[Fe(CN)_5]^{3-}$ and the free L. This can be explained in terms of (i) the σ donation of L to the metal, which makes the amine more positive, and better solvated with water molecules acting as donors; (ii) the larger degree of back-donation to the cyanides in the complex compared with $[Fe(CN)_5]^{3-}$, due to the electronic density provided by the amine, which makes more favorable the solvation of cyanides in the complex.

The diamine cases are more complicated, since there is an interplay between internal versus solvent hydrogen bonding, and solvation effects do not affect bond dissociation energies appreciably. However, the agreement with experiment is good. Considering the first solvation shell, the most stable structures for hydrazine and en complexes are closed and open conformations, respectively. For en, both structures turn out to be local minima in vacuum; this is not the case in the hydrazine complexes, for which the open structure was always found to collapse into the closed one.

Conclusions

We have shown that DFT techniques at the GGA level provide a useful tool in the investigation of the energetics and structure of $[Fe(CN)_5L]^{3-}$ with L an aliphatic mono- or diamine. We have also presented results obtained with a very simple model in which the complex was treated at the DFT level and the first solvation shell was modeled using classical potentials. By using this model we were able to interpret the trends in the dissociation enthalpy of these ligands.

The success of this model, which neglects long-range dielectric effects is due to the fact that since there is no charge separation in reaction (1) the most important solvent effect is related to first shell specific interactions. [9]

Acknowledgment This work was partially supported by the University of Buenos Aires and CONICET. D.A.E acknowledges Fundación Antorchas for financial support. D.A.E and J.A.O are members of the scientific staff of CONICET (National Scientific Council of Argentina).

References

1. Salahub DR, Zerner MC (1989) The challenge of d and f electrons, ACS Symposium Series 394. American Chemical Society, Washington, D.C.
2. Deeth DR (1995) Computational modelling of transition metal centers. In: Structure and bonding, Vol. 82. Springer, Berlin Heidelberg New York
3. (a) Salahub DR, Fournier R, Mlynarski P, Papai I., St-Amant A, Ushio J (1990). In: Labanowski J, Andzelm J (eds) Theory and applications of density functional approaches in chemistry. Springer, Berlin Heidelberg New York; (b) Ziegler T

(1991) Chem Rev 91:651; (c) Sosa C, Andzelm J, Elkin BC, Wimmer E, Dobbs KD, Dixon DA (1992) J Phys Chem 96:6630
4. Balzani V, Sabbatini N, Scandola F (1986) Chem Rev 86:319
5. (a) Ehlers AW, Frenking G (1994) J Am Chem Soc 116:1514; (b) Krogh-Jespersen K, Zhang X, Ding Y, Westbrook JD, Potena JA, Schugar HJ (1992) J Am Chem Soc 114:4345
6. (a) Li J, Schreckenbach G, Ziegler T (1995) J Am Chem Soc 117:486; (b) Daul C, Baerends EJ, Vernooijs P (1994) Inorg Chem 33:3538
7. For recent examples see (2000) Chem Rev 100 (2): issue devoted to computational transition metal chemistry
8. Estrin DA, Baraldo LM, Slep LD, Barja BC, Olabe JA (1996) Inorg Chem 35:3897
9. Hamra OY, Slep LD, Olabe JA, Estrin DA (1998) Inorg Chem 37:2033
10. (a) Toma HE, Takasugi MS (1983) J Solution Chem 12:547; (b) Toma HE, Takasugi MS (1989) J Solution Chem 18:575; (c) Timpson CJ, Bignozzi CA, Sullivan BP, Kober EM, Meyer TJ (1996) J Phys Chem 100:2915; (d) Slep LD, Baraldo LM, Olabe JA (1996) Inorg Chem 35:6327; (e) Waldhoer E, Kaim W, Olabe JA, Slep LD, Fiedler J (1997) Inorg Chem 36:2969
11. Estrin DA, Hamra OY, Paglieri L, Slep LD, Olabe JA (1996) Inorg Chem 35:6832
12. Macartney DH (1988) Rev Inorg Chem :101
13. Estrin DA, Corongiu G, Clementi E (1993) In: Clementi E (ed) METECC, methods and techniques in computational chemistry, Chapter 12. Stef, Cagliari
14. Kohn W, Sham LJ (1965) Phys Rev A 140:1133
15. Becke AD (1988) J Chem Phys 88:1053
16. (a) Sim F, Salahub D, Chin S, Dupuis M (1991) J Chem Phys 95:4317; (b) Sim F, St-Amant A, Papai Y. Salahub DR (1992) J Am Chem Soc 114:4391
17. Andzelm J, Radzio E, Salahub DR (1985) J Comput Chem 6:520
18. Vosko SH, Wilk L, Nusair M (1980) Can J Chem 58:1200
19. Becke AD (1988) Phys Rev A 38:3098
20. (a) Perdew PW (1986) Phys Rev B 33:8800; (b) Perdew PW (1986) Erratum. Phys Rev B 34:7406
21. Siegbahn PEM (1996) Adv Chem Phys 93:333
22. Wu JH, Reynolds CA (1996) J Am Chem Soc 118:14899
23. (a) Ho LL, MacKerell AD, Bash PA (1996) J Phys Chem 100:4466; (b) Eurenius KP, Chatfield DC, Brooks BR (1996) Int J Quant Chem 60:1189
24. Jorgensen WL, Chandrasekhar J, Madura JD, Impey RW, Klein ML (1983) J Chem Phys 79:926
25. Parise A, Piro OE, Castellano EE, Olabe JA Inorg Chim Acta in press
26. Bray MR, Deeth RJ, Paget VJ, Sheen PD (1996) Int J Quantum Chem 61:85
27. (1988) CRC handbook of chemistry and physics, 1st student edn. CRC Press, Boca Raton, Fla.
28. Lias SG, Liebman JF, Levin RD (1984) J Phys Chem Ref Data 13:696
29. (a)Katz NE, Aymonino PJ, Blesa MA, Olabe JA (1978) Inorg Chem 17:556; (b) Olabe JA, Gentil LA (1983) Transition Met Chem 8:65; (c) Katz NE, Blesa MA, Olabe JA, Aymonino PJ, J Chem Soc Dalton Trans (1978) 14:1603
30. Hoddenbagh JMA, Macartney DH (1986) Inorg Chem 25:9173
31. Stochel G, Chatlas J, Martinez P, van Eldik R (1992) Inorg Chem 31:5480
32. Burgess J, Patel MS (1993) J Chem Soc Faraday Trans 89:783
33. Li J, Schreckenbach G, Ziegler T (1994) J Phys Chem 98:4838
34. Stravrev KK, Zerner MC, Meer J (1995) J Am Chem Soc 117:8684